Wiley
Indoor Air
Volume 2024, Article ID 6816185, 17 pages
https://doi.org/10.1155/2024/6816185

WILEY

Research Article

Relationships between Electroencephalogram and Thermal Perception of Passenger in Winter Vehicle Compartments

Xin Xu,[1,2] **Lanping Zhao**,[3] **Yuxin Hu**,[2,3] **Qinyue Zheng**,[2,3] **Guomin Wu**,[2,3] **and Zhigang Yang**[1,2]

[1]*School of Automotive Studies, Tongji University, Shanghai, China*
[2]*Shanghai Key Lab of Vehicle Aerodynamics and Vehicle Thermal Management Systems, Shanghai, China*
[3]*Institute of Refrigeration and Cryogenic Engineering, School of Mechanical Engineering, Tongji University, Shanghai, China*

Correspondence should be addressed to Lanping Zhao; lanping_zhao@163.com

Received 19 October 2023; Revised 7 February 2024; Accepted 6 May 2024; Published 28 May 2024

Academic Editor: Faming Wang

The development of electric vehicles (EVs) has prompted a critical examination of the trade-off between range and human thermal comfort. Therefore, an accurate, real-time assessment of human thermal perception inside vehicles is important. This study investigates an electroencephalogram- (EEG-) based method for evaluating human thermal comfort in the vehicle passenger compartment. Under transient winter heating conditions, the study experimentally investigates the correlation between objective physiological parameters (skin temperature and electroencephalogram) and subjective human thermal perception. The results reveal distinct patterns in EEG signals corresponding to changes in thermal perception. Specifically, the δ rhythm exhibits a U-shape variation with increasing thermal perception, while the θ, α, β, and γ rhythms display an inverted U-shape variation. Differences in each frequency band across thermal comfort states in humans are greater than differences in the frequency band across thermal sensation states. Furthermore, the relative power of the θ rhythm emerges as the most effective in discerning the thermal perception state of the human body. The EEG signal characteristics of the T7 and T8 channels align more closely with human thermal sensation, whereas the AF4 channel excels at discriminating the state of human thermal comfort. The insights gained from this study serve as a foundation for evaluating human thermal perception in vehicles, enhancing human-vehicle interaction, and addressing challenges related to human thermal comfort and vehicle range.

1. Introduction

With urbanization, people increasingly spend more extended time traveling in vehicles, emphasizing the growing importance of ensuring thermal comfort for users within the vehicle's passenger compartment [1, 2]. To achieve this, heating, ventilation, and air conditioning (HVAC) systems create a comfortable thermal environment. In the context of energy consumption and carbon emissions, transportation accounts for a significant one-third share [3, 4]. As part of the global shift towards "dual carbon" (carbon neutral and peak carbon), electric vehicles (EVs) have emerged as a prominent trend. By 2040, it is projected that there will be approximately 548 million EVs worldwide, constituting around 32% of the global passenger car fleet [5]. Nevertheless, the transition to EVs presents novel challenges compared to conventional internal combustion engine (ICE) vehicles, which utilize the engine as a heat source to warm the passenger compartment during winter. In contrast, EVs solely rely on electrical energy to enhance thermal comfort within the vehicle interior, which may compromise driving range. Vehicle air conditioning systems, in general, account for about 20% of total vehicle energy consumption and up to 60% in urban areas and under severe conditions [6]. Therefore, the primary objective of the vehicle interior's thermal design is to provide optimal thermal comfort to occupants while minimizing energy usage [7].

Human thermal comfort is a prominent subject in the HVAC domain, and thermal comfort is defined as the degree of satisfaction with the current thermal environment [8]. Over the past decades, numerous thermal comfort evaluation models and criteria have been proposed, with

Fanger's predicted mean vote (PMV) and predicted percentage of dissatisfaction (PPD) being the most commonly utilized ones [9]. However, these models are based on controlled steady-state uniform thermal environments, while the thermal conditions within the passenger compartment of an automobile are transient and nonuniform. Heat transfer by radiation and conduction accounts for a greater proportion in a vehicle than heat exchange in a building, due to the greater proportion of glass area. Solar radiation enters the cabin by transmission or absorption. The human body exchanges heat by conduction with the seats and steering wheel in contact. The operating air-conditioning system generates an uneven heat flow field in the automobile passenger compartment, so the amount of convective heat exchange varies among the driver's and passenger's body parts. Due to the directional nature of solar shortwave direct radiation, this radiation can only be received by certain parts of the body. All of which contribute to the differences between the indoor environments of automobiles and buildings. Consequently, several studies have highlighted significant biases in using the PMV-PPD model to predict human thermal comfort in automotive settings [10, 11]. Owing to the variability in human thermal comfort, there is a potential for enhancing the predictive efficacy of thermal comfort evaluation models based on environmental parameters. Consequently, scholars began to focus more on exploring the correlation between physiological parameters and the subjective evaluation of the human body. Wyon introduced the concept of equivalent homogeneous temperature while evaluating the thermal environment in vehicles using warm body dummies. This concept integrates the sensible heat exchange between the human body and the environment (convective and radiative). It proves to be effective in assessing human thermal comfort in nonuniform thermal environments within automobiles [12]. Moreover, the Berkeley Thermal Comfort Evaluation Model can assess human thermal comfort in transient nonuniform thermal environments. This model comprehensively analyzes the correlation between skin temperature, core temperature, thermal sensation, and thermal comfort based on 109 human experiments conducted under controlled conditions in a room with nonuniform and transient thermal conditions. Consequently, BCEM establishes models for local thermal sensation, local thermal comfort, total thermal sensation, and total thermal comfort of the human body [13]. Presently, standards such as EN ISO 14505/1 [14], EN ISO 14505/2 [15], EN ISO 14505/3 [16], and EN ISO 14505/4 [17] are available for evaluating the thermal environment of vehicles. These standards provide guidelines for thermal stress assessment principles and methods, determination of equivalent temperature, real-life experiments, and numerical approaches, respectively. However, it is essential to note that the models proposed in these standards were primarily developed based on research experience in construction [18].

Prior studies have focused on extracting features from physiological signals, such as EEG, ECG, skin temperature, and core temperature, to predict human thermal comfort [19]. Human beings can perceive external stimuli because the interior of the skin epidermis contains numerous receptor vesicle cells, of which Ruffini vesicles are temperature receptors. These vesicles encode the stimuli received into electrical signals that are transmitted through nerve fibers to the dorsal root ganglia, then to the spinal cord, and finally to the human brain. Skin temperature serves as an indicator of heat transfer between the body and the environment. At the same time, EEG provides insights into the central nervous system's response, and ECG offers indications of the autonomic nervous system response [20]. Nonetheless, physiological parameters like skin temperature, core temperature, and heat flow, essential for existing thermal comfort evaluation models, often prove challenging to execute in real-time within the thermal environment of an automobile occupant compartment. In this context, EEG signals have garnered particular attention due to their direct characterization of the nervous system's activity. By employing spectral estimation on continuous EEG recordings, it becomes possible to calculate the power of various rhythms within five brain frequency bands, extracting information about the individual's mental states. Recent human studies utilizing positron emission tomography (PET) or functional magnetic resonance imaging (fMRI) have demonstrated significant effects on specific areas of the cerebral cortex in response to thermal skin stimulation [21]. Consequently, the power spectral densities of different EEG signal rhythms are commonly employed to determine an individual's thermal comfort, tension, or relaxation levels.

Air temperature is widely recognized as the primary environmental factor influencing human thermal perception. Various studies have investigated the influence of EEG characteristics under different temperatures in controlled environments. Yao et al. conducted experiments collecting thermal sensation voting (TSV) and EEG data from subjects with closed eyes at four different temperatures. The results indicated a significant increase in the spectral power of β-band EEG during occurrences of thermal discomfort, while the spectral power of θ and δ bands decreased [22]. Mansi et al. measured EEG under cold, neutral, and warm conditions, observing an increase in α relative power under warm conditions and an increase in β and γ power under cold sensations [23]. Lang et al. explored the effect of a high-temperature environment (39°C) on EEG, noting a significant increase in δ rhythm relative power and a decrease in β rhythm relative power compared to the neutral environment [24]. In addition to air temperature (Ta), changes in relative humidity (RH), wind speed (Va), and radiation temperature can also affect EEG signals. Pan et al. simulated three airflow condition levels (0, 0.5, and 1.0 m/s) in the laboratory to study the impact on EEG signals, finding a significant increase in relative β and δ power of the F3 channel in the absence of airflow (0 m/s) compared to 0.5 and 1.0 m/s [25]. An increase in radiation temperature led to an increase in the relative power of β and α, along with frontal EEG asymmetry forming an inverted "U"-shaped response curve [26]. When RH was 70%, δ relative power increased significantly with increasing Ta. In contrast, α, β, and θ relative powers decreased significantly, suggesting that EEG can objectively and immediately measure the environment's impact on perception and facilitate the

understanding of thermal comfort mechanisms [27]. While previous studies were predominantly based on uniform thermal environments, few studies have focused on human body thermal comfort and EEG signals in transient thermal environments. Son and Chun applied EEG in a temperature step experiment to assess thermal pleasure, observing an increase in Fz relative θ frequency in the frontal midline but a decrease in β power in the frontal, central, and parietal midlines, with no significant effect on α and γ [28]. When people experienced thermal discomfort with a gradual temperature increase or decrease, the relative powers of α, β, θ, and δ all increased significantly [29]. Scholars have recognized the close relationship between EEG and cognitive behavior through previous studies, leading to research on driving behavior. Gwak et al. designed a thermal environment to enhance arousal levels and feelings of thermal comfort [30]. Studies of drivers in the thermal environment of automotive cockpits demonstrated the suitability of photoplethysmography (PPG) and electroencephalography (EEG) for evaluating concentration, pressure, and thermal comfort [31]. These studies on driving behavior were conducted in simulated indoor environments. Machine learning techniques have proven effective for EEG analysis and have been extensively used for passive real-time measurement. Shan et al. used EEG pattern recognition based on machine learning to investigate the interaction between occupants and buildings under various environmental conditions [32, 33]. The study demonstrated an association between human responses collected through questionnaires and EEG frontal lobe asymmetry. Wu et al. [34] conducted a series of studies on brain-computer interface- (BCI-) based closed-loop control systems for room temperature. Firstly, they measured and analyzed the characteristics of EEG signals in different thermal comfort states and observed the differences in different bands as well as different electrodes. Then, an online system was developed based on the thermal sensory discrimination model (TSDM) established by the integrated learning method [35], and the generalization ability of the model was improved by a convolutional neural network (CNN) [36].

The physiological parameter of EEG signals holds advantages for measurements in thermal environments within automobile occupant compartments, and its high temporal resolution property allows for better correlation with changes in human thermal comfort state during transient changes in thermal environments. However, the existing studies mentioned above have some limitations:

(1) Thermal comfort holds paramount significance in the domain of architecture. Consequently, numerous studies have investigated EEG signals in laboratory settings with controlled, steady-state, and uniform conditions. However, these studies lack representation of the typical transient and nonuniform thermal environment experienced in the passenger compartments of automobiles

(2) Studies on transient thermal environments have mainly compared and analyzed the differences in EEG signals before and after environmental changes. However, they must thoroughly explore how the EEG signals change with the thermal environment throughout the process

(3) The characteristics of EEG signals in different thermal comfort states remain inconclusive, and diverse studies have produced varying results, possibly due to the distinct characteristics of the thermal environment and the cognitive behavior of the subjects

This study assessed EEG signals and human thermal perception within the winter passenger compartment under varying heating conditions. The aim was to analyze the potential of relative power and entropy values of EEG signals in reflecting the thermal comfort experienced by both the driver and passengers in the automobile. Additionally, we identified the most suitable EEG channels and their corresponding rhythms for evaluating human thermal sensation and comfort. The findings of this study serve as a theoretical foundation for future assessments of human thermal comfort in vehicles based on EEG signals. Moreover, they offer insights for optimizing in-vehicle air-conditioning systems and promoting energy-saving practices in the human-vehicle interaction mode.

Table 1: Demographic information of the subjects (values are means ± standard deviation).

Gender	Quantity	Age (year-old)	Height (cm)	Weight (kg)
Male	10	24.3 ± 1.7	173.8 ± 5.1	72.7 ± 9.7
Female	10	23.0 ± 1.3	165.2 ± 4.5	59.3 ± 8.4

2. Methods

2.1. Experiment

2.1.1. Subjects. Twenty healthy college students (ten males and ten females) were recruited as human subjects who signed an informed consent form before the experiments. Table 1 lists the basic information of the subjects, with age, height, and weight expressed as mean ± standard deviation. Subjects were introduced to the experimental procedure and instructed to complete the subjective evaluation questionnaire before the formal experiment. Subjects were asked to wear typical local clothing (sweatpants and long-sleeve sweatshirts), corresponding to a clothing level of 0.74 clo [8]. During the experiment, subjects were asked to sit quietly in a relaxed posture in the driver and passenger seats, in addition to avoiding caffeine, alcohol, smoking, and vigorous physical activity for 12 hours prior to each experiment.

2.1.2. Experimental Conditions. The experiment was conducted in February 2023 in an indoor parking lot at Tongji University in Shanghai, China. The space in the parking lot was large enough to maintain a constant ambient temperature of about 10°C around the outside of the experimental vehicle during the experiment. The experimental vehicle was a SAIC Volkswagen Lavida with automatic air conditioning and seat heating, and the internal dimensions of the passenger compartment of the car were 1.88 m ∗ 1.36 m ∗ 0.96 m. Three

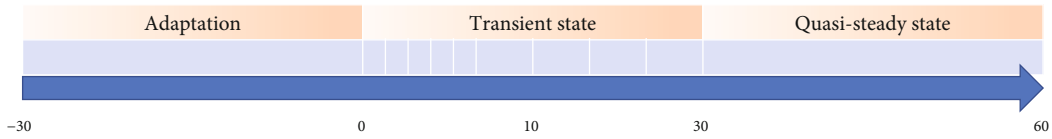

(a)

(b)

Figure 1: Experimental procedures and scenario diagram.

typical conditions were designed for the transient warming process in the passenger compartment in winter: automatic air conditioning set to 26°C, automatic air conditioning set to 22°C with electric seat heating, automatic air conditioning set to 26°C with electric seat heating, and electric seat heating set to a constant temperature of 33°C.

2.1.3. Experimental Procedure. Before the experiment started, subjects were asked to rest for about 30 minutes in the preparation room to reach a neutral thermal equilibrium state. The preparation room is a temperature- and humidity-controlled environmental chamber with a set temperature of 26°C and a relative humidity of 50%. During the adaptation, subjects entered the experimental vehicle, arranged thermocouples, and wore an EEG signal acquisition device with the help of the experimental staff, and this time was about 10 minutes. Then, the warming experiment started, and the transient heating condition in the vehicle lasted for one hour, with two participants in each experiment sitting in the driver and passenger positions. The subjects' skin temperature and EEG signals were measured during the experiment. Local and overall subjective thermal sensation and thermal comfort questionnaires were conducted. Since the experimental study considered the changes in human EEG signals in a transient automobile thermal environment, the questionnaire can be categorized into a transient and quasi-steady state according to the experimental time, with the first thirty minutes being the transient questionnaire and the second thirty minutes being the steady state questionnaire. The questionnaire was filled out every two minutes for the first ten minutes, every five minutes from ten to thirty minutes, and every ten minutes for the steady-state questionnaire for the last thirty minutes. The specific experimental flow is shown in Figure 1(a). Figure 1(b) shows the experimental scenario diagram.

2.2. Measurements

2.2.1. Thermal Environment Parameters in the Vehicle Passenger Compartment. The heat exchange through conduction, convection, and radiation in the passenger compartment of a vehicle affects thermal comfort, so it is necessary to measure the internal surface and air temperatures in the vehicle's passenger compartment. As shown in Figure 2(a) [37], thermocouple measurement points 1-3 measured the interior surface temperature, and measurement points 4-15 measured the interior air temperature. Measurement points 1-3 are the dashboard temperature, windshield temperature, and roof temperature. Temperatures 4-7 are driver, copilot (copilot occupies the right front seat), and rear passenger breathing points air temperatures, respectively. Temperatures 8-11 are the air temperatures around the abdomen of the driver, codriver, and passenger. Temperatures at measurement points 12-15 are the air temperatures around the torso of the driver, copilot, and passenger. Measurement points 16-17 are the air conditioning air supply parameter measurement points in the passenger compartment of the automobile, measuring the air supply temperature and air supply speed on the driver's side and the passenger's side, respectively. The sampling interval of the ambient temperature data acquisition system is set to 1 second.

2.2.2. Human Physiological Parameters. To study the thermal comfort of humans in the passenger cabin, 18 thermocouples were used to measure the skin temperatures of different body parts of the experimental subjects, including the head, chest, abdomen, upper arm, lower arm, hand, thigh, hip, calf, and foot, as shown in Figure 2(b). The measurement points of the thermocouples were fixed in the middle of each body part with medical tape. The sampling interval of the skin temperature data acquisition system was set to 1 second.

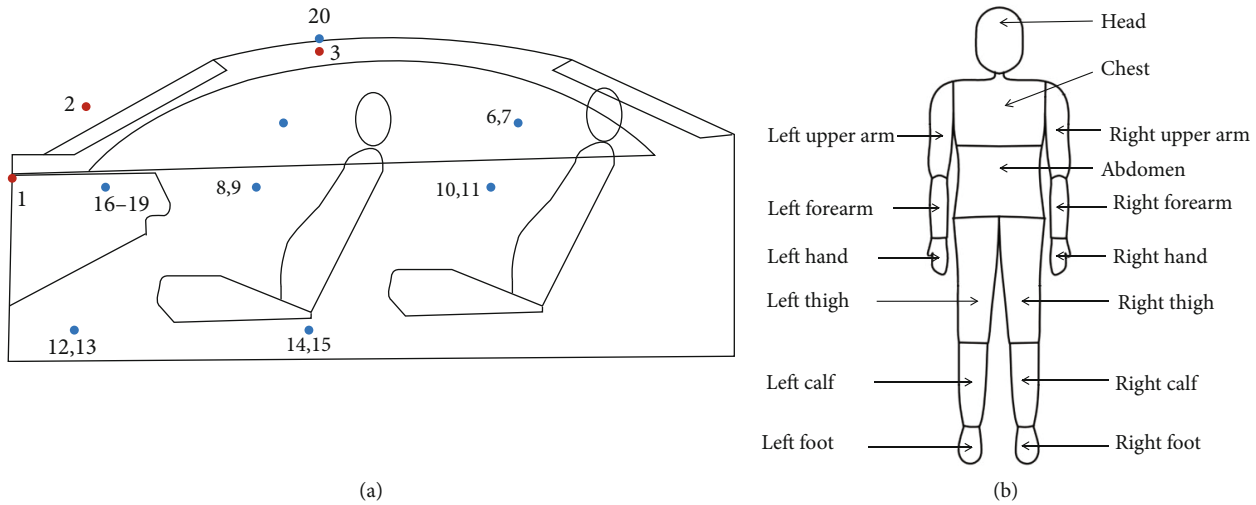

Figure 2: Measurement positions of thermocouples in the experiment: (a) for cabin interior wall and air temperature and (b) for skin temperatures of experimental personnel.

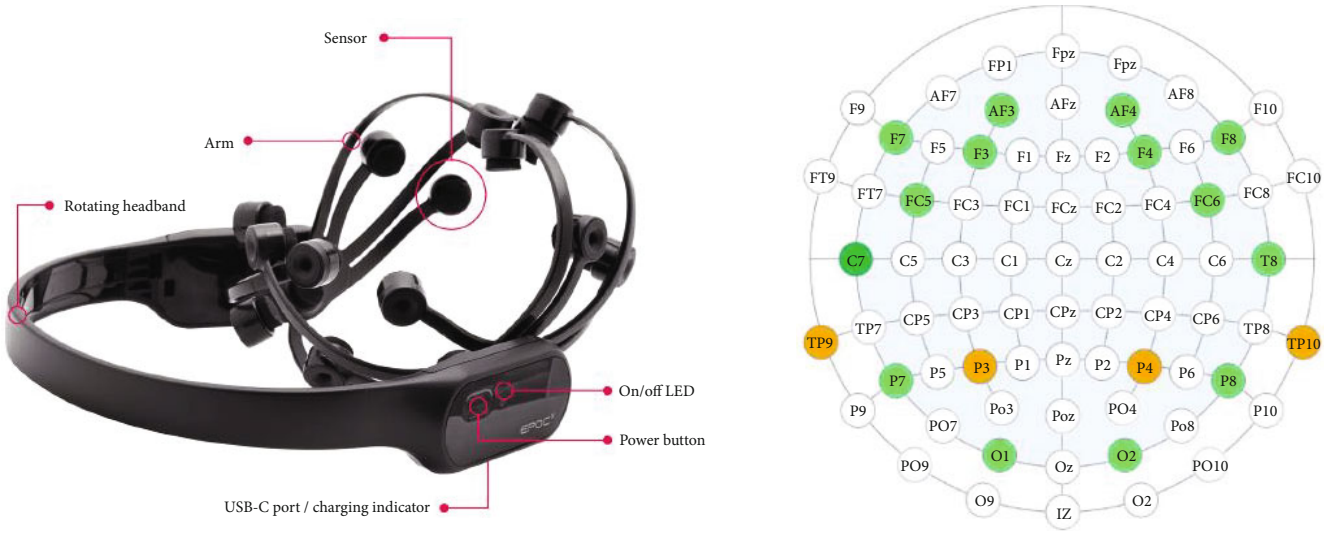

Figure 3: EEG recording system and channel location.

Amplitude and rhythm are typical characteristics of EEG signals and characterize, to some extent, the subject's physiological state. There are five primary EEG waves, which are distinguished by different frequency ranges. These rhythms ranging from low to high frequencies are called δ (0.5-4 Hz), θ (4-8 Hz), α (8-13 Hz), β (13-30 Hz), and γ (30-45 Hz), respectively [38]. In this experiment, EEG signals were measured by Emotiv EpocX. The channel schematic is shown in Figure 3, where the measurement channels are green and the reference channels are orange. According to the International 10-20 system [39], it has 14 channels located in four central regions of the brain: frontal (AF 3, F7, F3, FC 5, FC 6, F4, F8, and AF 4), temporal (T7, T8), occipital (O1, O2), and parietal (P7, P8). CMS/DRL references are at P3/P4. TP9 and TP10 are alternate reference channels. The EpocX has a sampling frequency of 128 Hz and sends the measured EEG signals to a computer via Bluetooth. All felt pads on top of the sensor must be well moistened with a saline solution before use. After data collection, all the data were imported into MATLAB for further processing. The EEG signals were measured for 40 minutes because some subjects reported that the EEG signal collector caused discomfort when worn for too long.

2.2.3. Subjective Evaluation Questionnaire. Compared with the building environment, the thermal environment in the passenger compartment of the car has nonuniform characteristics, so the subjects reach a more extreme thermal sensation and thermal comfort state, so this experimental questionnaire uses a 9-point subjective evaluation scale as shown in Figure 4. During the experiment, the subjects filled in the electronic questionnaire in the form of a cell phone, which included the local thermal sensation and thermal comfort and the overall thermal sensation and thermal comfort of the human body.

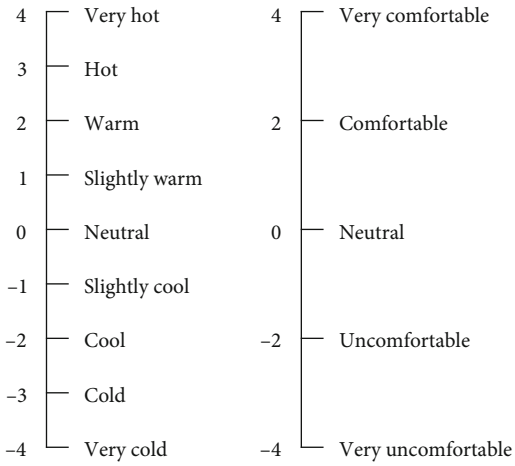

Figure 4: Scales of thermal sensation and thermal comfort.

2.3. Data Processing and Statistics. The average skin temperature was calculated using the DuBois 7-point formula.

$$\begin{aligned} \mathrm{MST}_{\mathrm{Hardy/DuBois(7\,points)}} = {} & 0.07t_{\mathrm{sk,forehead}} + 0.35t_{\mathrm{sk,abdomen}} \\ & + 0.14t_{\mathrm{sk,forearm}} + 0.05t_{\mathrm{sk,hand}} \\ & + 0.19t_{\mathrm{sk,thigh}} + 0.13t_{\mathrm{sk,calf}} \\ & + 0.07t_{\mathrm{sk,foot}}. \end{aligned} \tag{1}$$

The EEG data were preprocessed by the EEGLAB toolbox (version 2022.1), widely used in MATLAB. The raw EEG signal was imported into the EEGLAB toolbox. First, high-pass filtered at 0.5 Hz to remove DC offset and low-frequency skin potential artifacts and then low-passed at 45 Hz to remove high-frequency noise. The amorphous artifacts were then manually removed by observing the data. The remaining artifacts, such as blinking and muscle activity, were removed by decomposing the EEG signal into its maximum independent components via an independent component analysis (ICA) algorithm and then removing the artifactual components. The artifact-free continuous data is then segmented into 60-second periods. The power spectrum analysis of the EEG signals for each rhythm was performed by the band power function in MATLAB. Shannon entropy was also used to analyze the uncertainty of the EEG signal. The relative energy share of each rhythm and the Shannon entropy formed the basis for the subsequent analysis as a characteristic of the EEG signal, where the Shannon entropy is calculated, as shown in Equation (2). All statistical work on the data was performed in SPSS25. Correlations between EEG signals of different rhythms of different channels and heat perception were analyzed using Pearson's correlation. A one-way ANOVA was used to analyze the energy share of different rhythms of EEG signals under different thermal perceptions.

$$H(x) = -c\sum_{i=0}^{m} p(x_i)\,\ln\,(p(x_i)). \tag{2}$$

3. Results

The Results show the air supply parameters, environmental parameters, human parameters (mean skin temperature and EEG signals), and subjective thermal perception under different working conditions. Correlation analysis and statistical analysis between EEG signals and subjective thermal perception were also performed.

3.1. Air Supply Parameters. Figure 5 shows the average air supply conditions by experimental working conditions, including the average air supply temperature and air supply speed. By comparing the differences in the air supply conditions under each condition, we find that the control strategy of the automatic air conditioning in the experimental vehicle is to change the air supply temperature rather than the air supply speed according to the different set targets. In Figure 5(a), we can see that the air supply temperature of the automatic air conditioning set to 22°C plus the electric heating condition has been maintained between 30 and 33°C, while the initial air supply temperature of the two conditions at 26°C exceeds 40°C. With or without electric heating conditions in the first 30 minutes of the air supply temperature difference may be due to the experimental car being located in the ambient temperature caused by, but as can be seen in the 30 minutes after the two are almost the same, it can be considered that the thermal environment of the car is needed to achieve the set target. In terms of air delivery speed, there was little difference between the three conditions in the first 30 minutes, while after 30 minutes, the air delivery speed of the automatic air conditioner set to 22°C was smaller than that of 26°C.

3.2. Environmental Parameters. Figure 6 shows the wall and air temperatures in the passenger compartment by experimental conditions. Figures 6(a), 6(b), and 6(c) show the wall temperature change curves for the automatic air conditioning setting of 26°C, the automatic air conditioning setting of 22°C with seat heating, and the automatic air conditioning setting of 26°C with seat heating. Figures 6(d), 6(e), and 6(f) show the air temperature change curves for the corresponding conditions. Wall temperatures are measurement points 1-3 in Figure 2(a). Air temperatures are averaged for face height at measurement points 4-7, abdomen height at measurement points 8-11, and foot height at measurement points 12-15. By comparing the different heating conditions, we can see that the thermal environment parameters in the car are mainly affected by the air conditioning parameters, and the electric heating cushion has less influence than the HVAC. Among the wall surface temperatures, the warming rate and steady-state equilibrium temperature of the dashboard and roof are higher than those of the windshield. Regarding air temperature, as the experimental vehicle winter automatic air conditioning air supply adopts the face air supply and foot air supply strategies, the air temperature at the foot position is the highest, followed by the face, and the lowest at the abdomen. Under the steady state condition, the air temperature of the feet reached 32-33°C under the working condition of the automatic air conditioning setting

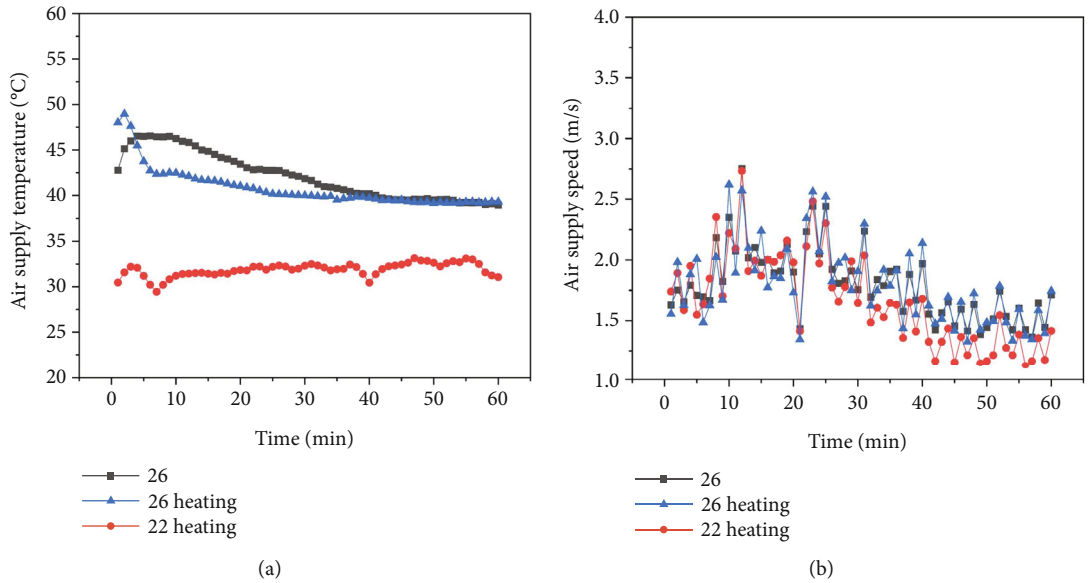

Figure 5: Air supply parameters: (a) air supply temperature and (b) air supply speed.

of 26°C, and the air temperature of the abdomen and face was around 30°C. Comparing the wall and air temperature, we found that the air temperature change in each condition is close to the quasisteady state before and after 20 minutes, while the wall temperature stabilization is slower than the air temperature stability after 40 minutes to approach the quasisteady state, which is caused by the heat capacity characteristics of the solid wall.

3.3. Physiological Parameters. From the results in Figure 7, we can see the curve of the average human skin temperature in the car's passenger compartment during the experiment. From the data in the figure, we can see that, compared with the condition of automatic air conditioning set at 26°C, the average skin temperature of the human body under the condition of an electric-heated cushion at 26°C rises faster. In the first 40 minutes, electric heating can make the average skin temperature difference of 0.5°C, while the skin temperature under the two conditions is close at 55 minutes. With automatic air conditioning set at 26°C working conditions, an hour of warming time makes the average human skin temperature rise about 3.5°C. Compared with automatic air conditioning set at 22°C with electric heating cushion working conditions, the temperature rise is only 1.5°C. The reason for this is that the temperature setting of the automatic air conditioning affects the air supply conditions in the passenger compartment of the car, and the more significant temperature difference enhances convective heat transfer, which in turn affects the average skin temperature.

The changes in energy percentage and Shannon entropy over time of EEG signals with different rhythms under three working conditions are demonstrated in Figure 8, from which we can see that the EEG signal is a very fluctuating temporal signal. Regarding the relative energy share, the EEG signal is a physiological signal dominated by low frequency, and the energy share of the δ-band EEG signal in the initial state is above 85%. In terms of time, the δ-rhythm of the EEG signal decreases during the 40-minute experiment, while the energy share of the other four rhythmic EEG signals increases with time. Comparing the three conditions, we find that there are apparent differences in the α-rhythms and entropy of the three experimental conditions, and the α-rhythms of the EEG signals of the subjects under the condition of automatic air-conditioning set at 26°C with point-heating cushions have a higher energy ratio than the other two conditions. Their entropy values are also more remarkable than those of the other two conditions.

3.4. Thermal Perception of Subjects. As we can see from Figure 9, the subjective thermal sensation and thermal comfort effects of the two operating conditions of automatic air conditioning at 26 degrees Celsius and 22 degrees Celsius with electric heating are relatively close. From the graph, we can also see that even under the same environmental conditions, the differences between subjects are apparent, with a standard deviation of about 1 for thermal sensation and about 2 for thermal comfort.

3.5. Correlation Analysis. Pearson's correlation coefficient was used to correlate the EEG signals of each rhythm and the Shannon entropy value for different electrodes in order to analyze the effect of heat perception on the EEG signals of different channels. Colors indicate a significant correlation, red indicates a positive correlation, and green indicates a negative correlation. Figure 10 shows that the EEG signals of δ-rhythms have opposite correlations with other rhythm EEG signals and entropy values with heat perception. The EEG signal δ rhythm is positively correlated with thermal sensation, and other EEG signal rhythms and entropy values are negatively correlated. The correlation of EEG signals with thermal comfort was the opposite of thermal sensation, with a negative correlation of δ-rhythms and a positive correlation of other EEG signal features. In addition, it was found that the energy share and entropy value of the gamma

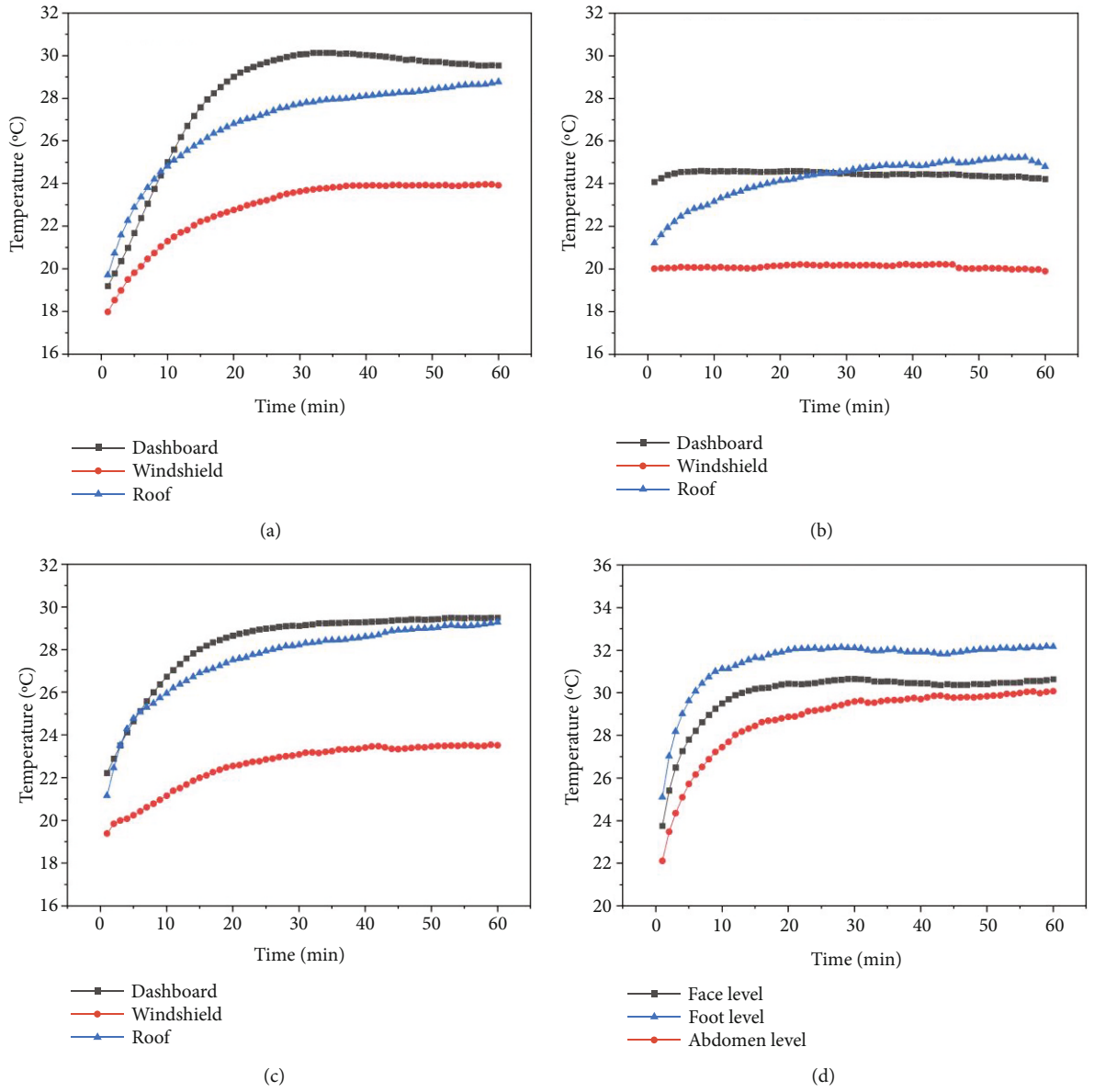

Figure 6: Continued.

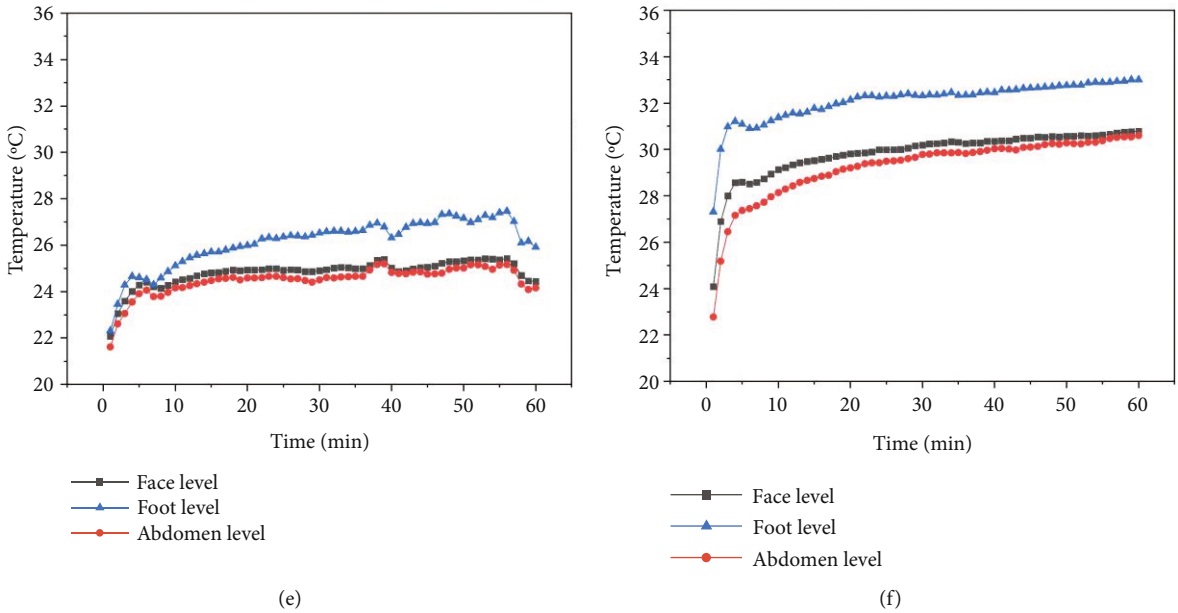

Figure 6: Environmental parameters: the wall temperature of (a) auto ac 26°C, (b) auto ac 22°C with seat heating, and (c) auto ac 26°C with seat heating and the air temperature of (d) auto ac 26°C, (e) auto ac 22°C with seat heating, and (f) auto ac 26°C with seat heating.

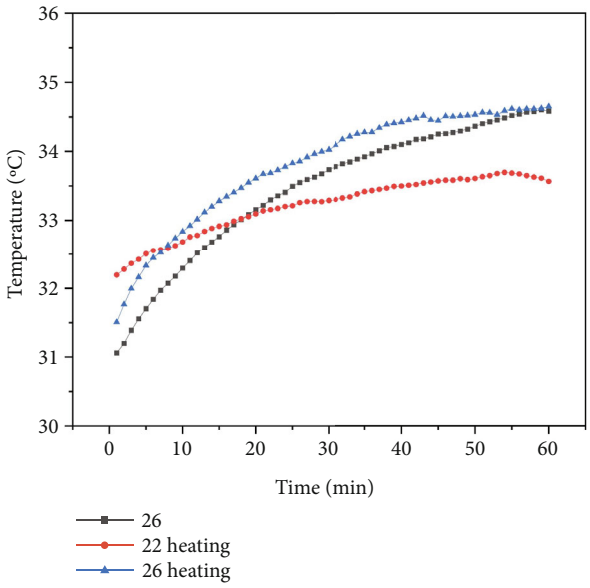

Figure 7: Mean skin temperature.

rhythm in the EEG signal characteristics were better correlated with thermal sensation than thermal comfort. Only the entropy values of the EEG signals of four channels, AF3, AF4, F3, and F4, were significantly correlated with thermal comfort.

3.6. Statistical Analysis. Whether the differences in EEG signals are due to the thermal environment or different states of human thermal perception, the global EEG signals were first analyzed, and here, the human thermal perception was reclassified by classifying human thermal sensation -4 to -2 as cold, -1 to +1 as neutrality, and +2 to +4 as hot. Similarly, human thermal comfort -4 to -2 is classified as uncomfortable, -1 to +1 as neutral, and +2 to +4 as comfortable. ANOVA was done for each rhythm of EEG signals, and then post hoc analysis was performed to compare the EEG signal characteristics under different thermal sensations and thermal comfort states. As shown in Figure 11, by comparing the energy share of each rhythm of EEG signals under different thermal sensations, we found that the energy share of δ-rhythm EEG signals in the neutral thermal sensation state is the lowest, and the energy share of other rhythms is higher than that of the cold and hot states. Furthermore, all EEG signal rhythms in the thermal neutral and hot states are significantly different, with p values less than 0.001. The results of the available experimental data indicate that only gamma waves in the cold state are different from the thermal neutral, and theta bands are significantly different from the hot state. By comparing the energy share of each rhythm of the EEG signals in different thermal comfort states, we found a similar pattern to that of thermal sensation. The energy share of the δ rhythm in the neutral thermal comfort state is smaller than in the comfortable and uncomfortable states. In addition, all the EEG signal rhythms in the neutral thermal comfort state were significantly different from those in the comfortable and uncomfortable states, with a p value of less than 0.001. In addition, only the theta-band comfortable and uncomfortable states showed significant differences, which can be used to determine whether the subjects were comfortable or not.

For thermal sensation, only the beta wave of the T7 channel and the alpha wave of the T8 channel showed significant differences in all three thermal sensation states. As for thermal comfort, 31 out of 70 EEG signal features in all 14 channels with five rhythms per channel showed significant differences among the three thermal comfort states. Among them, 20 (20/31) were in the frontal region, 4 (4/31) in the parietal lobe, 1 in the occipital lobe, and 6 in the temporal

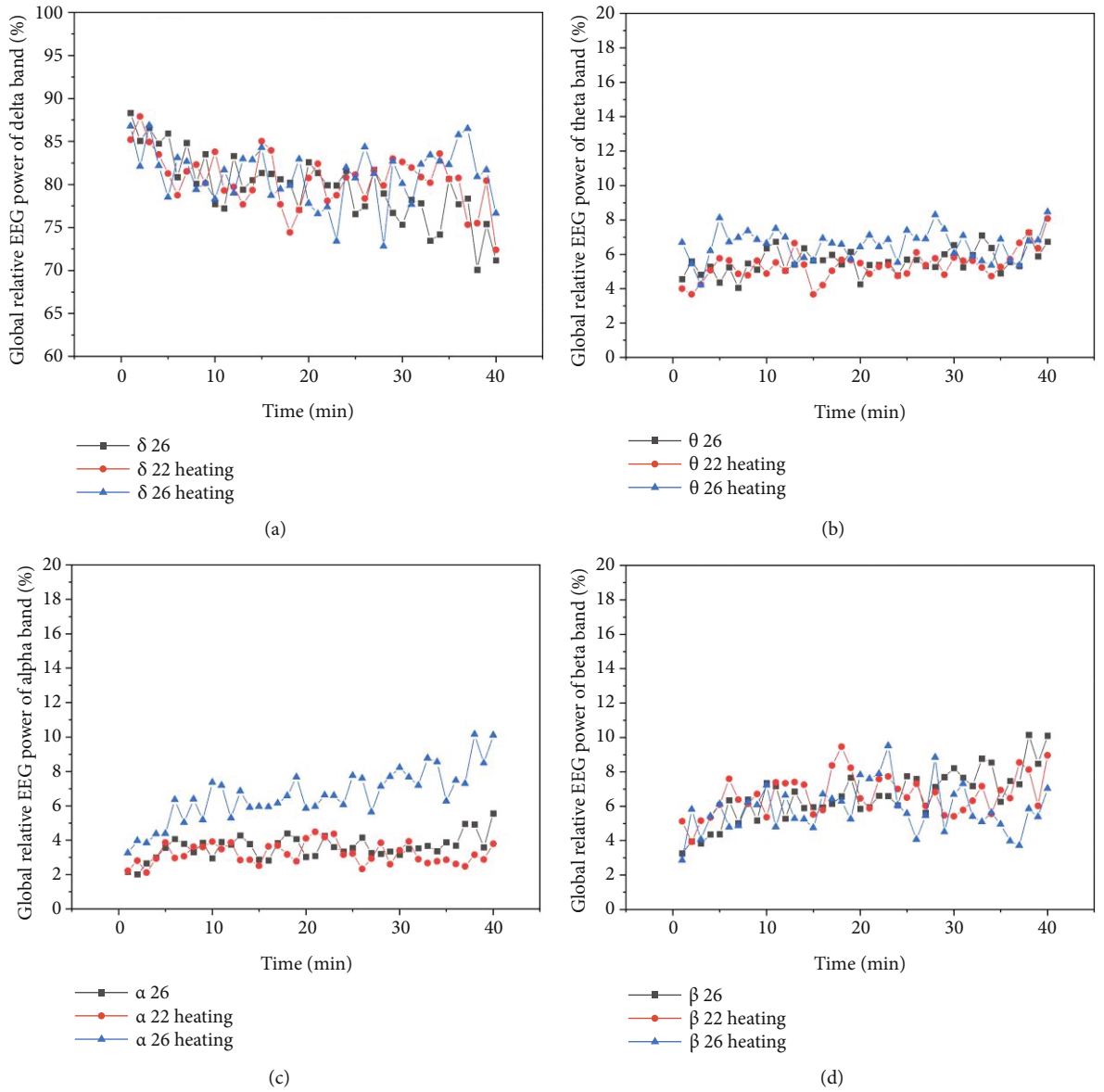

Figure 8: Continued.

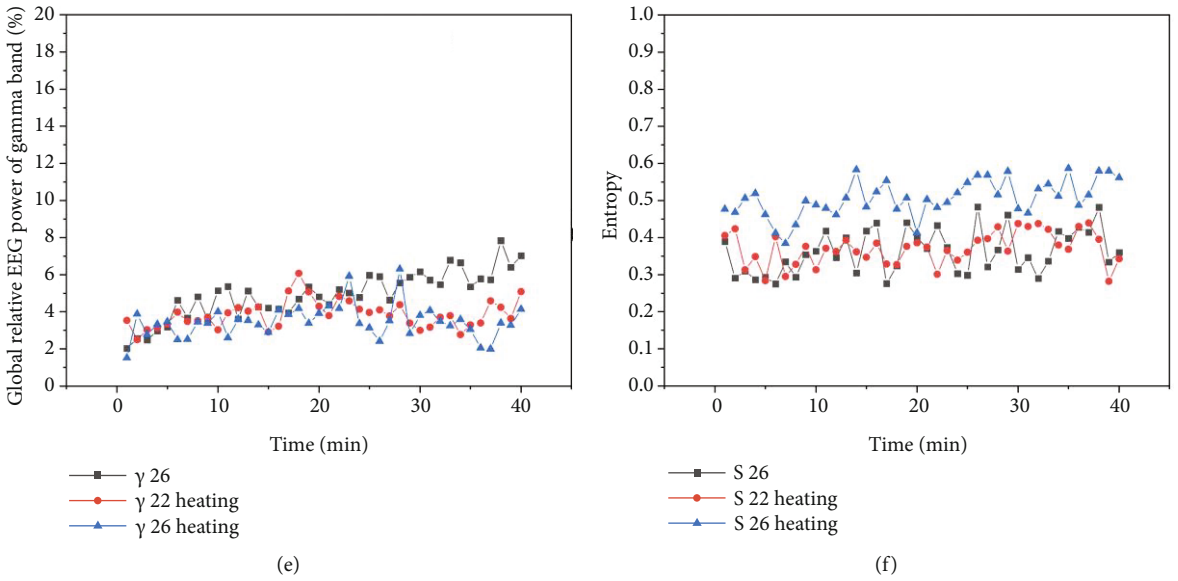

Figure 8: EEG signal characterization.

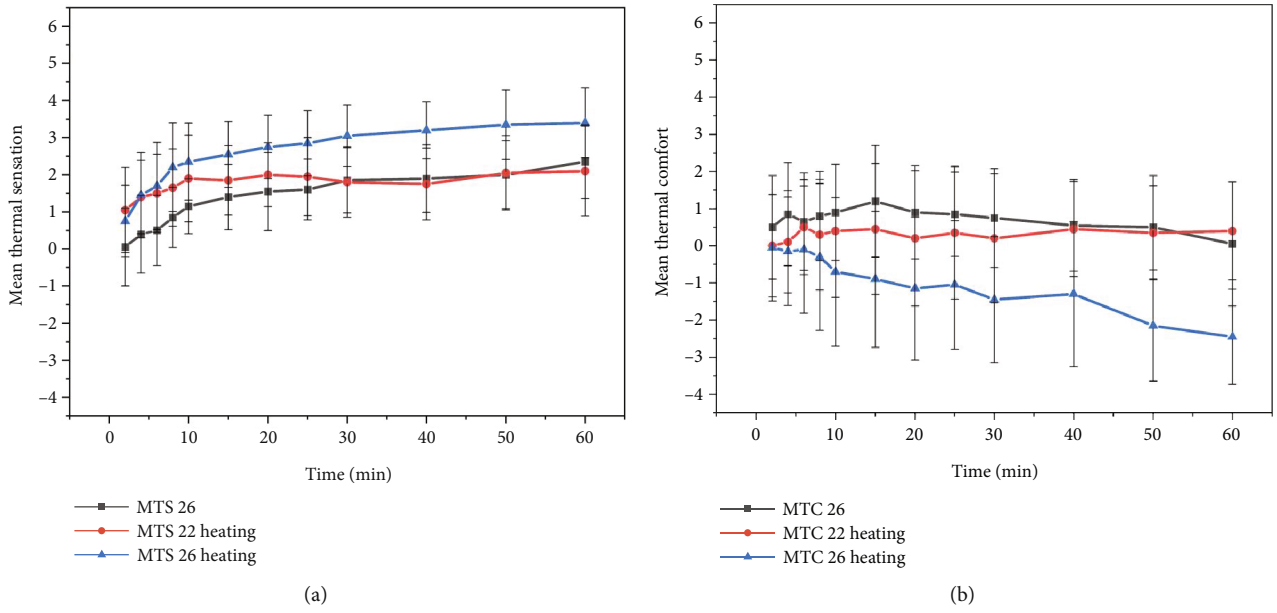

Figure 9: Human thermal sensation and thermal comfort.

lobe. The energy share of EEG signals in five bands of the AF4 channel showed significant differences in all three thermal comfort states.

4. Discussion

This study conducted three typical heating conditions in the car occupant's cabin during winter. The research findings revealed that the relative energy ratio of EEG signals in the δ band gradually decreased with increasing experiment time, while other bands exhibited an upward trend. Subsequently, we employed univariate analysis of variance to examine the average EEG rhythm energy ratio under different heat perceptions. The relative power of the δ rhythm in EEG exhibits a U-shaped variation with an increase in heat perception, while the θ, α, β, and γ rhythms demonstrate an inverse-U-shaped trend. Wu et al. [34] posited that when subjects experience a sensation of heat, there is an increase in low-frequency energy and a decrease in high-frequency energy. This improvement in the "hot" sensation at low frequencies and the inhibition at high frequencies corresponded to a decrease in cognitive activity and a decline in cognitive performance, aligning with our observations. Regarding the relationship between EEG signals and thermal comfort, the research results of Son and Chun [28] and Han and Chun [29] suggested that thermal comfort leads to an increase in

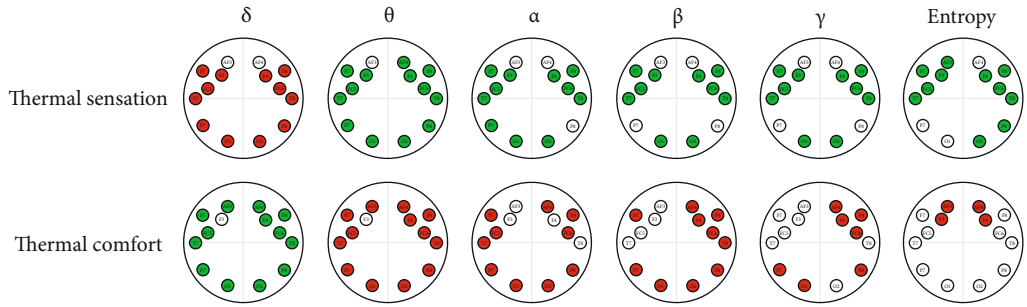

Figure 10: Correlation analysis.

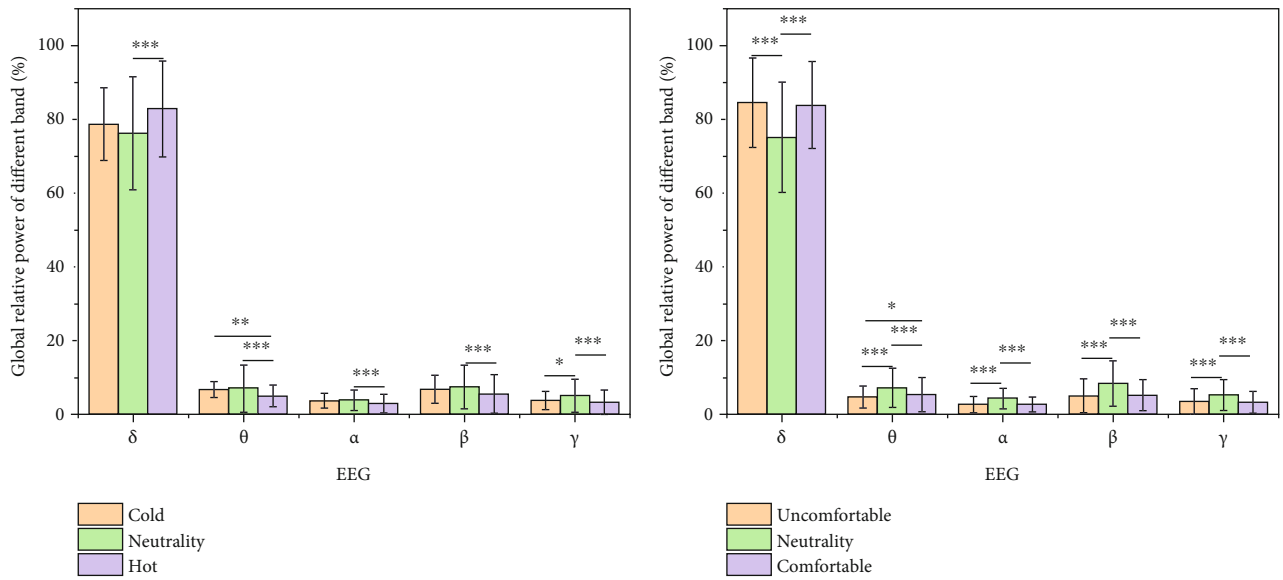

Figure 11: Relationship of EEG signals to thermal sensation and thermal comfort, $^{*}P < 0.05$, $^{**}P < 0.01$, $^{***}P < 0.001$.

the relative energy proportion of theta rhythm and a decrease in beta waves. Deviation from our results can be attributed, in part, to the distinct classification ranges of EEG rhythms and variations in thermal comfort evaluation scales, which may exert specific influences. Moreover, due to experimental conditions, the number of votes for the subjective thermal sensation of feeling cold in the car occupant's cabin with the air conditioning turned on during winter is relatively small. Consequently, the difference in EEG signals between the experimental results for cold thermal sensation and neutral thermal sensation states was minimal, with the relative energy ratio of the global EEG signal displaying significant differences only in the gamma band. Significant differences exist between cold sensation and thermal sensation in the theta band, and the post hoc analysis results based on thermal comfort states reveal notable distinctions among EEG signals in all bands, specifically under neutral thermal comfort conditions as well as in comfortable and uncomfortable states. Furthermore, only the theta band exhibits significant differences between comfortable and uncomfortable states, indicating that the theta band appears to be the most effective EEG feature for evaluating human thermal sensation and thermal comfort states. Several studies have also highlighted the reliability of theta-band EEG in representing human thermal comfort [27, 28].

The ANOVA analysis of EEG signals for each channel revealed that differences in EEG signals resulting from variations in human thermal comfort had a more pronounced impact than thermal sensation. The experimental data indicated significant differences in thermal sensation only for the beta rhythm of T7 and the alpha rhythm of T8. In contrast, for thermal comfort, 31 out of 70 EEG signal features across all 14 channels, with five rhythms per channel, displayed significant differences among the three thermal comfort states. These significant differences encompassed 20 features in the frontal lobe, 4 in the parietal lobe, 1 in the occipital lobe, and 6 in the temporal lobe. Additionally, the energy share of EEG signals in the five bands from the AF4 channel exhibited significant differences among all three thermal comfort states. Determining which channel's EEG signal characteristics best reflect the thermal perception state of the human body. Different studies have yielded diverse results. Some research has indicated that the parietal and frontal lobes are more sensitive to thermal environments, which aligns with our experimental findings [40]. The disparities in outcomes among different experiments can be attributed to the subjects'

Table 2: Relative power of local EEG signals in different thermal perception states (mean ± SD).

EEG channel	EEG band	Relative power for thermal sensation			Relative power for thermal comfort		
		Ratings of the cold	Ratings of the neutral	Ratings of the hot	Ratings of being thermally uncomfortable	Ratings of being thermally neutrality	Ratings of being thermally comfortable
AF3	δ				$0.828 \pm 0.211^{B,C}$	0.795 ± 0.17	0.797 ± 0.216
	θ	0.084 ± 0.039	0.076 ± 0.072^{C}	0.069 ± 0.049	$\mathbf{0.059 \pm 0.047^{B,C}}$	$\mathbf{0.083 \pm 0.062^{C}}$	$\mathbf{0.07 \pm 0.063}$
	α	0.047 ± 0.039^{B}	0.031 ± 0.034	0.035 ± 0.043	0.031 ± 0.043^{B}	0.036 ± 0.036	0.035 ± 0.043
	β				0.051 ± 0.086^{C}	0.055 ± 0.069^{C}	0.061 ± 0.085
	γ				0.031 ± 0.051^{C}	0.031 ± 0.044^{C}	0.038 ± 0.058
F7	δ	0.861 ± 0.079	0.842 ± 0.138^{C}	0.891 ± 0.088	0.905 ± 0.086^{B}	0.833 ± 0.127^{C}	0.897 ± 0.088
	θ	0.069 ± 0.031	0.066 ± 0.075	0.052 ± 0.038^{C}	$\mathbf{0.042 \pm 0.033^{B,C}}$	$\mathbf{0.073 \pm 0.065^{C}}$	$\mathbf{0.053 \pm 0.053}$
	α	0.023 ± 0.016^{C}	0.025 ± 0.025^{C}	0.016 ± 0.016	0.014 ± 0.014^{B}	0.027 ± 0.024^{C}	0.014 ± 0.013
	β	0.031 ± 0.028	0.041 ± 0.046^{C}	0.026 ± 0.033	0.024 ± 0.03^{B}	0.042 ± 0.048^{C}	0.022 ± 0.023
	γ	0.016 ± 0.014^{B}	0.027 ± 0.035^{C}	0.015 ± 0.021	0.016 ± 0.025^{B}	0.025 ± 0.033^{C}	0.014 ± 0.016
F3	δ	0.795 ± 0.148^{B}	0.709 ± 0.227^{C}	0.802 ± 0.185	$\mathbf{0.802 \pm 0.179^{B,C}}$	$\mathbf{0.702 \pm 0.225^{C}}$	$\mathbf{0.846 \pm 0.155}$
	θ	0.066 ± 0.036	0.081 ± 0.073^{C}	0.062 ± 0.046	0.058 ± 0.048^{B}	0.085 ± 0.063^{C}	0.056 ± 0.054
	α	0.039 ± 0.032	0.052 ± 0.046^{C}	0.037 ± 0.038	$\mathbf{0.037 \pm 0.038^{B,C}}$	$\mathbf{0.055 \pm 0.047^{C}}$	$\mathbf{0.026 \pm 0.026}$
	β	0.064 ± 0.055^{B}	0.094 ± 0.089^{C}	0.063 ± 0.072	$\mathbf{0.063 \pm 0.067^{B,C}}$	$\mathbf{0.099 \pm 0.091^{C}}$	$\mathbf{0.045 \pm 0.055}$
	γ	0.037 ± 0.036^{B}	0.065 ± 0.069^{C}	0.037 ± 0.046	$\mathbf{0.041 \pm 0.046^{B,C}}$	$\mathbf{0.061 \pm 0.065^{C}}$	$\mathbf{0.028 \pm 0.045}$
FC5	δ	0.816 ± 0.109^{C}	0.786 ± 0.16^{C}	0.868 ± 0.115	0.868 ± 0.123^{B}	0.794 ± 0.148^{C}	0.874 ± 0.117
	θ	0.073 ± 0.032^{C}	0.07 ± 0.074^{C}	0.048 ± 0.036	$\mathbf{0.044 \pm 0.035^{B,C}}$	$\mathbf{0.07 \pm 0.062^{C}}$	$\mathbf{0.052 \pm 0.055}$
	α	0.034 ± 0.023^{C}	0.034 ± 0.029^{C}	0.021 ± 0.021	0.02 ± 0.021^{B}	0.034 ± 0.028^{C}	0.018 ± 0.017
	β	0.052 ± 0.044	0.066 ± 0.062^{C}	0.039 ± 0.045	0.04 ± 0.046^{B}	0.064 ± 0.06^{C}	0.035 ± 0.039
	γ	0.026 ± 0.022^{B}	0.045 ± 0.049^{C}	0.024 ± 0.032	$\mathbf{0.029 \pm 0.04^{B,C}}$	$\mathbf{0.04 \pm 0.043^{C}}$	$\mathbf{0.022 \pm 0.029}$
T7	δ	0.686 ± 0.19^{C}	0.716 ± 0.211^{C}	0.822 ± 0.165	0.819 ± 0.18^{B}	0.717 ± 0.2^{C}	0.84 ± 0.146
	θ	0.057 ± 0.022^{C}	0.061 ± 0.072^{C}	0.035 ± 0.027	$\mathbf{0.032 \pm 0.025^{B,C}}$	$\mathbf{0.058 \pm 0.06^{C}}$	$\mathbf{0.042 \pm 0.051}$
	α	0.042 ± 0.025^{C}	0.039 ± 0.034^{C}	0.024 ± 0.026	0.022 ± 0.025^{B}	0.041 ± 0.034^{C}	0.02 ± 0.021
	β	$\mathbf{0.137 \pm 0.098^{B,C}}$	$\mathbf{0.106 \pm 0.094^{C}}$	$\mathbf{0.072 \pm 0.077}$	$\mathbf{0.073 \pm 0.083^{B,C}}$	$\mathbf{0.11 \pm 0.092^{C}}$	$\mathbf{0.059 \pm 0.062}$
	γ	0.079 ± 0.056^{C}	0.079 ± 0.075^{C}	0.048 ± 0.052	$\mathbf{0.054 \pm 0.064^{B,C}}$	$\mathbf{0.075 \pm 0.067^{C}}$	$\mathbf{0.04 \pm 0.042}$

Table 2: Continued.

EEG channel	EEG band	Relative power for thermal sensation			Relative power for thermal comfort		
		Ratings of the cold	Ratings of the neutral	Ratings of the hot	Ratings of being thermally uncomfortable	Ratings of being thermally neutrality	Ratings of being thermally comfortable
P7	δ	0.803 ± 0.123	0.784 ± 0.197^{C}	0.828 ± 0.185	$\mathbf{0.863 \pm 0.161^{B,C}}$	$\mathbf{0.758 \pm 0.213^{C}}$	$\mathbf{0.829 \pm 0.152}$
	θ	0.059 ± 0.031^{C}	0.068 ± 0.069^{C}	0.042 ± 0.036	$\mathbf{0.041 \pm 0.047^{B,C}}$	$\mathbf{0.062 \pm 0.056^{C}}$	$\mathbf{0.05 \pm 0.046}$
	α	0.032 ± 0.029	0.037 ± 0.041^{C}	0.027 ± 0.032	$\mathbf{0.021 \pm 0.025^{B,C}}$	$\mathbf{0.042 \pm 0.043^{C}}$	$\mathbf{0.026 \pm 0.028}$
	β				$\mathbf{0.044 \pm 0.064^{B,C}}$	$\mathbf{0.082 \pm 0.085^{C}}$	$\mathbf{0.056 \pm 0.059}$
	γ				0.033 ± 0.055^{B}	0.056 ± 0.061^{C}	0.04 ± 0.045
O1	δ	0.827 ± 0.107^{B}	0.739 ± 0.223^{C}	0.814 ± 0.175	0.842 ± 0.152^{B}	0.72 ± 0.219^{C}	0.829 ± 0.17
	θ	0.05 ± 0.025	0.058 ± 0.043^{C}	0.043 ± 0.035	0.039 ± 0.031^{B}	0.06 ± 0.041^{C}	0.042 ± 0.039
	α	0.028 ± 0.019^{B}	0.045 ± 0.041^{C}	0.035 ± 0.035	0.027 ± 0.026^{B}	0.052 ± 0.043^{C}	0.031 ± 0.033
	β	0.06 ± 0.046^{B}	0.091 ± 0.088^{C}	0.068 ± 0.072	0.054 ± 0.061^{B}	0.102 ± 0.088^{C}	0.062 ± 0.069
	γ	0.035 ± 0.027^{B}	0.068 ± 0.076^{C}	0.041 ± 0.048	0.039 ± 0.053^{B}	0.067 ± 0.069^{C}	0.037 ± 0.043
O2	δ	0.782 ± 0.167^{B}	0.713 ± 0.208^{C}	0.811 ± 0.17	0.826 ± 0.157^{B}	0.703 ± 0.204^{C}	0.833 ± 0.161
	θ	0.063 ± 0.032^{C}	0.076 ± 0.071^{C}	0.046 ± 0.036	0.044 ± 0.039^{B}	0.073 ± 0.061^{C}	0.046 ± 0.05
	α	0.037 ± 0.03^{B}	0.053 ± 0.043^{C}	0.038 ± 0.038	0.032 ± 0.031^{B}	0.059 ± 0.045^{C}	0.033 ± 0.034
	β	0.072 ± 0.068	0.095 ± 0.081^{C}	0.067 ± 0.067	0.058 ± 0.061^{B}	0.104 ± 0.081^{C}	0.058 ± 0.062
	γ	0.045 ± 0.05^{B}	0.063 ± 0.066^{C}	0.038 ± 0.043	$\mathbf{0.04 \pm 0.049^{B,C}}$	$\mathbf{0.062 \pm 0.061^{C}}$	$\mathbf{0.031 \pm 0.036}$
P8	δ	0.787 ± 0.151	0.766 ± 0.185^{C}	0.814 ± 0.172	0.839 ± 0.153^{B}	0.737 ± 0.194^{C}	0.837 ± 0.148
	θ	0.066 ± 0.038^{C}	0.08 ± 0.082^{C}	0.044 ± 0.034	0.047 ± 0.044^{B}	0.072 ± 0.069^{C}	0.047 ± 0.052
	α	0.037 ± 0.03	0.04 ± 0.034^{C}	0.036 ± 0.036	0.029 ± 0.03^{B}	0.05 ± 0.04^{C}	0.028 ± 0.026
	β				0.051 ± 0.059^{B}	0.091 ± 0.08^{C}	0.056 ± 0.057
	γ				0.033 ± 0.042^{B}	0.051 ± 0.054^{C}	0.033 ± 0.037
T8	δ	0.708 ± 0.133^{C}	0.717 ± 0.223^{C}	0.813 ± 0.161	$\mathbf{0.813 \pm 0.169^{B,C}}$	$\mathbf{0.71 \pm 0.212^{C}}$	$\mathbf{0.842 \pm 0.131}$
	θ	0.07 ± 0.027^{C}	0.063 ± 0.073^{C}	0.045 ± 0.035	0.045 ± 0.04^{B}	0.062 ± 0.061^{C}	0.047 ± 0.052
	α	$\mathbf{0.055 \pm 0.03^{B,C}}$	$\mathbf{0.041 \pm 0.035^{C}}$	$\mathbf{0.033 \pm 0.033}$	$\mathbf{0.031 \pm 0.032^{B,C}}$	$\mathbf{0.047 \pm 0.037^{C}}$	$\mathbf{0.024 \pm 0.022}$
	β	0.111 ± 0.057^{C}	0.103 ± 0.099^{C}	0.069 ± 0.07	0.066 ± 0.069^{B}	0.11 ± 0.098^{C}	0.055 ± 0.051
	γ	0.057 ± 0.031	0.077 ± 0.087^{C}	0.04 ± 0.042	$\mathbf{0.045 \pm 0.054^{B,C}}$	$\mathbf{0.072 \pm 0.078^{C}}$	$\mathbf{0.033 \pm 0.032}$

Table 2: Continued.

EEG channel	EEG band	Relative power for thermal sensation			Relative power for thermal comfort		
		Ratings of the cold	Ratings of the neutral	Ratings of the hot	Ratings of being thermally uncomfortable	Ratings of being thermally neutrality	Ratings of being thermally comfortable
FC6	δ	0.828 ± 0.099^{B}	0.776 ± 0.168^{C}	0.871 ± 0.11	0.877 ± 0.103^{B}	0.78 ± 0.164^{C}	0.879 ± 0.101
	θ	0.067 ± 0.032^{C}	0.072 ± 0.072^{C}	0.048 ± 0.033	$\mathbf{0.044 \pm 0.032^{B,C}}$	$\mathbf{0.071 \pm 0.06^{C}}$	$\mathbf{0.054 \pm 0.054}$
	α	0.035 ± 0.025^{C}	0.037 ± 0.031^{C}	0.023 ± 0.024	0.021 ± 0.021^{B}	0.039 ± 0.032^{C}	0.019 ± 0.017
	β	0.048 ± 0.034^{B}	0.069 ± 0.067^{C}	0.037 ± 0.044	0.035 ± 0.036^{B}	0.07 ± 0.069^{C}	0.031 ± 0.032
	γ	0.022 ± 0.016^{B}	0.046 ± 0.052^{C}	0.021 ± 0.025	$\mathbf{0.024 \pm 0.03^{B,C}}$	$\mathbf{0.041 \pm 0.048^{C}}$	$\mathbf{0.017 \pm 0.021}$
F4	δ	0.713 ± 0.183	0.671 ± 0.234^{C}	0.759 ± 0.221	$\mathbf{0.786 \pm 0.201^{B,C}}$	$\mathbf{0.671 \pm 0.227^{C}}$	$\mathbf{0.736 \pm 0.247}$
	θ	0.081 ± 0.031^{C}	0.082 ± 0.072^{C}	0.062 ± 0.044	0.059 ± 0.046^{B}	0.082 ± 0.061^{C}	0.064 ± 0.057
	α	0.052 ± 0.03	0.053 ± 0.039^{C}	0.044 ± 0.042	0.039 ± 0.04^{B}	0.058 ± 0.042^{C}	0.041 ± 0.035
	β	0.097 ± 0.079	0.11 ± 0.093^{C}	0.083 ± 0.087	$\mathbf{0.071 \pm 0.079^{B,C}}$	$\mathbf{0.113 \pm 0.091^{C}}$	$\mathbf{0.09 \pm 0.094}$
	γ	0.057 ± 0.055^{B}	0.085 ± 0.092^{C}	0.053 ± 0.067	$\mathbf{0.046 \pm 0.054^{B,C}}$	$\mathbf{0.076 \pm 0.082}$	$\mathbf{0.071 \pm 0.098}$
F8	δ	0.868 ± 0.08	0.842 ± 0.143^{C}	0.901 ± 0.081	$\mathbf{0.918 \pm 0.072^{B,C}}$	$\mathbf{0.836 \pm 0.133^{C}}$	$\mathbf{0.899 \pm 0.083}$
	θ	0.064 ± 0.031	0.067 ± 0.072^{C}	0.048 ± 0.032	$\mathbf{0.039 \pm 0.03^{B,C}}$	$\mathbf{0.069 \pm 0.06^{C}}$	$\mathbf{0.055 \pm 0.051}$
	α	0.025 ± 0.019^{C}	0.026 ± 0.026^{C}	0.016 ± 0.016	0.013 ± 0.014^{B}	0.028 ± 0.026^{C}	0.015 ± 0.013
	β	0.03 ± 0.026	0.041 ± 0.05^{C}	0.023 ± 0.029	0.019 ± 0.023^{B}	0.043 ± 0.051^{C}	0.021 ± 0.021
	γ	0.014 ± 0.012^{B}	0.025 ± 0.036^{C}	0.012 ± 0.017	0.012 ± 0.016^{B}	0.025 ± 0.035^{C}	0.011 ± 0.013
AF4	δ				$\mathbf{0.851 \pm 0.146^{B,C}}$	$\mathbf{0.754 \pm 0.195^{C}}$	$\mathbf{0.803 \pm 0.23}$
	θ	0.084 ± 0.032^{C}	0.076 ± 0.072^{C}	0.065 ± 0.043	$\mathbf{0.055 \pm 0.042^{B,C}}$	$\mathbf{0.083 \pm 0.061^{C}}$	$\mathbf{0.067 \pm 0.057}$
	α				$\mathbf{0.027 \pm 0.029^{B,C}}$	$\mathbf{0.046 \pm 0.04^{C}}$	$\mathbf{0.035 \pm 0.044}$
	β				$\mathbf{0.042 \pm 0.055^{B,C}}$	$\mathbf{0.076 \pm 0.082^{C}}$	$\mathbf{0.061 \pm 0.095}$
	γ				$\mathbf{0.026 \pm 0.036^{B,C}}$	$\mathbf{0.042 \pm 0.05}$	$\mathbf{0.035 \pm 0.059}$

Post hoc analyses of the EEG signals with different rhythms of each channel were performed to obtain the EEG signal characteristics that best characterize human thermal perception. The mean and standard deviation of the relative energy share of the different channel EEG signal rhythms corresponding to different cortical locations are given in Table 2. Values are given only for those features for which there is a significant difference, and bold indicates that there is a significant difference for all three thermal sensory states. Thermal sensation cases A, B, and C represent cold, neutral, and hot; thermal comfort cases A, B, and C represent uncomfortable, neutral, and comfortable. Superscript-labeled letters represent significant differences from that condition.

environmental conditions and cognitive behaviors, both of which influence the characteristics of EEG signals. Consequently, these findings should not be solely interpreted as an effect of heat perception.

Notably, the experiment was conducted under winter-warming conditions, leading to the subjects experiencing a range of thermal sensations from cold to hot. Subsequent investigations during summer cooling conditions will allow us to ascertain whether the changes in EEG signals are primarily influenced by the duration of the experiment or by the subjects' subjective thermal perception. Furthermore, exploring whether the variations in EEG frequency are due to the experiment's duration or shifts in human thermal comfort requires further investigation. Moreover, the experiments were conducted under parking conditions, and the EEG signal characteristics of the subjects closely resembled their subjective thermal perception, which was characterized by passenger characteristics. Given the close connection between the physiological features of EEG signals and the type of cognitive activity in the subjects, it is reasonable to expect that drivers' driving behavior could impact these results. Thus, additional research is warranted to ascertain the feasibility of developing a model to evaluate the thermal comfort of both drivers and passengers in the vehicle passenger compartment based on EEG signals.

5. Conclusions

This study experimentally investigated a new EEG-based approach to enhance driver-passenger interaction with the in-vehicle thermal environment. Correlations were established between objective human physiological parameters, including skin temperature, electroencephalogram, and subjective evaluations, through power spectral analysis with entropy values. The primary conclusions are as follows:

(i) The relative power of the δ frequency band showed a U-shaped variation in response to changes in thermal perception. In contrast, the θ, α, β, and γ rhythms exhibited an inverted U-shaped pattern

(ii) The difference in electroencephalogram between different thermal comfort states is more significant than the difference between different thermal sensation states

(iii) Among the various EEG frequency bands, the relative energy share of the θ band most accurately characterized the subjects' subjective thermal sensation and thermal comfort state

(iv) The EEG signal characteristics of the T7 and T8 channels demonstrated better responsiveness to the thermal sensation state of the human body. In contrast, the AF4 channel exhibited superior capability in differentiating the thermal comfort state of the human body

Future research will explore the correlation between human thermal comfort and EEG signals during summer cooling within the car's passenger compartment. In addition, we will delve into the effects of various cognitive behaviors on EEG signals during the experiment. Furthermore, our focus will be extended to the investigation of driving conditions to explore the possibility of building a comprehensive model based on an electroencephalogram for assessing the thermal comfort of drivers and passengers.

Data Availability

The data are available from the corresponding author on reasonable request.

Disclosure

The authors disclosed receipt of the following financial support for the research, authorship, and/or publication of this article. A preprint has previously been published [1].

Conflicts of Interest

The authors declare that they have no conflicts of interest.

Acknowledgments

This work is supported by the National Key R&D Program of China (2022YFE0208000), the Fundamental Research Funds for the Central Universities.

References

[1] X. Xu, L. Zhao, Y. Hu, Q. Zheng, G. Wu, and Z. Yang, "Relationships between EEG and thermal perception in winter vehicle passenger compartments," https://ssrn.com/abstract=4538303.

[2] A. Lajunen, Y. Yang, and A. Emadi, "Review of cabin thermal management for electrified passenger vehicles," *IEEE Transactions on Vehicular Technology*, vol. 69, no. 6, pp. 6025–6040, 2020.

[3] L. Capuano, *International energy outlook 2018 (IEO2018) for center for strategic and international studies*, U.S. Energy Information Administration, 2018.

[4] Eurostat, *Greenhouse gas emission statistics — emission inventories*, European Comission, 2019.

[5] BloombergNEF, *Electric vehicle outlook 2019*, 2019.

[6] A. Lahlou, F. Ossart, E. Boudard, F. Roy, and M. Bakhouya, "A dynamic programming approach for thermal comfort control in electric vehicles," in *2018 IEEE Vehicle Power and Propulsion Conference (VPPC)*, Chicago, IL, USA, August 2018.

[7] G. J. Marshall, C. P. Mahony, M. J. Rhodes, S. R. Daniewicz, N. Tsolas, and S. M. Thompson, "Thermal management of vehicle cabins, external surfaces, and onboard electronics: an overview," *Engineering*, vol. 5, no. 5, pp. 954–969, 2019.

[8] ASHRAE, *Thermal environmental conditions for human occupancy*, American Society of Heating, Refrigerating and Air-Conditioning Engineers, Atlanta, GA, 2013.

[9] P. O. Fanger, "Thermal comfort: analysis and applications in environmental engineering," in *Abstr. in World Textile Abstracts. Applied Ergonomics. 1972*, p. 244, Danish Technical Press, Copenhagen, Denmark, 1970.

[10] J. G. Ingersoll, T. G. Kalman, L. M. Maxwell, and R. J. Niemiec, "Automobile passenger compartment thermal comfort model - part ii: human thermal comfort calculation," in *SAE Technical Paper Series*, February 1992.

[11] K. Matsunaga, F. Sudo, S. I. Tanabe, and T. L. Madsen, "Evaluation and measurement of thermal comfort in the vehicles with a new thermal manikin," in *SAE Technical Paper Series*, November 1993.

[12] D. P. Wyon, "Use of thermal manikins in environmental ergonomics," *Scandinavian Journal of Work Environment & Health*, vol. 15, Supplement 1, pp. 84–94, 1989.

[13] H. Zhang, *Human thermal sensation and comfort in transient and non-uniform thermal environments*, University of California Berkeley, 2003.

[14] ISO standards, 14505-1 I, *Ergonomics of the thermal environment-evaluation of thermal environments in vehicles part 1: principles and methods for assessment of thermal stress*, ISO standards, 2007, ISO 14505-1: 2007.

[15] ISO standards, 14505-2 I, *Ergonomics of the thermal environment-evaluation of thermal environments in vehicles — part 2: determination of equivalent temperature*, ISO standards, 2006, ISO 14505-2: 2006.

[16] ISO standards, 14505-3 I, *Ergonomics of the thermal environment-evaluation of thermal environments in vehicles part 3: evaluation of thermal comfort using human subjects*, ISO standards, 2006, ISO 14505-3: 2006.

[17] ISO standards, 14505-4 I, *Ergonomics of the thermal environment — evaluation of thermal environments in vehicles — part 4: determination of the equivalent temperature by means of a numerical manikin*, ISO standards, 2021, SO 14505-4: 2021.

[18] P. Dancă, F. Bode, I. Năstase, C. V. Croitoru, and A. Meslem, "Experimental and numerical study of the air distribution inside a car cabin," *E3S Web of Conferences*, vol. 85, article 02014, 2019.

[19] Y. Yao, Z. Lian, W. Liu, C. Jiang, Y. Liu, and H. Lu, "Heart rate variation and electroencephalograph – the potential physiological factors for thermal comfort study," *Indoor Air*, vol. 19, no. 2, pp. 93–101, 2009.

[20] S. A. Mansi, G. Barone, C. Forzano et al., "Measuring human physiological indices for thermal comfort assessment through wearable devices: a review," *Measurement*, vol. 183, article 109872, 2021.

[21] K. Kanosue, N. Sadato, T. Okada et al., "Brain activation during whole body cooling in humans studied with functional magnetic resonance imaging," *Neuroscience Letters*, vol. 329, no. 2, pp. 157–160, 2002.

[22] Y. Yao, Z. Lian, W. Liu, and Q. Shen, "Experimental study on physiological responses and thermal comfort under various ambient temperatures," *Physiology & Behavior*, vol. 93, no. 1-2, pp. 310–321, 2008.

[23] S. A. Mansi, I. Pigliautile, M. Arnesano, and A. L. Pisello, "A novel methodology for human thermal comfort decoding via physiological signals measurement and analysis," *Building and Environment*, vol. 222, article 109385, 2022.

[24] X. Lang, P. Wargocki, and W. Liu, "Investigating the relation between electroencephalogram, thermal comfort, and cognitive performance in neutral to hot indoor environment," *Indoor Air*, vol. 32, no. 1, Article ID e12941, 2022.

[25] L. Pan, H. Zheng, and T. Li, "Effects of the indoor environment on EEG and thermal comfort assessment in males," *Building and Environment*, vol. 228, article 109761, 2023.

[26] H. Niu, Y. Zhai, Y. Huang, X. Wang, and X. Wang, "Investigating the short-term cognitive abilities under local strong thermal radiation through EEG measurement," *Building and Environment*, vol. 224, article 109567, 2022.

[27] M. Zhu, W. Liu, and P. Wargocki, "Changes in EEG signals during the cognitive activity at varying air temperature and relative humidity," *Journal of Exposure Science & Environmental Epidemiology*, vol. 30, no. 2, pp. 285–298, 2020.

[28] Y. J. Son and C. Chun, "Research on electroencephalogram to measure thermal pleasure in thermal alliesthesia in temperature step-change environment," *Indoor Air*, vol. 28, no. 6, pp. 916–923, 2018.

[29] J. Han and C. Chun, "Differences between EEG during thermal discomfort and thermal displeasure," *Building and Environment*, vol. 204, article 108220, 2021.

[30] J. Gwak, M. Shino, K. Ueda, and M. Kamata, "Effects of changes in the thermal factor on arousal level and thermal comfort," in *2015 IEEE International Conference on Systems, Man, and Cybernetics*, Hong Kong, China, October 2015.

[31] Y. Shin, G. Im, K. Yu, and H. Cho, "Experimental study on the change in driver's physiological signals in automobile HVAC system under full load condition," *Applied Thermal Engineering*, vol. 112, pp. 1213–1222, 2017.

[32] X. Shan, E. H. Yang, J. Zhou, and V. W. C. Chang, "Human-building interaction under various indoor temperatures through neural-signal electroencephalogram (EEG) methods," *Building and Environment*, vol. 129, pp. 46–53, 2018.

[33] X. Shan and E. H. Yang, "Supervised machine learning of thermal comfort under different indoor temperatures using EEG measurements," *Energy and Buildings*, vol. 225, article 110305, 2020.

[34] M. Wu, H. Li, and H. Qi, "Using electroencephalogram to continuously discriminate feelings of personal thermal comfort between uncomfortably hot and comfortable environments," *Indoor Air*, vol. 30, no. 3, pp. 534–543, 2020.

[35] X. He, M. Wu, H. Li, S. Liu, B. Liu, and H. Qi, "Real-time regulation of room temperature based on individual thermal sensation using an online brain-computer interface," *Indoor Air*, vol. 32, no. 9, Article ID e13106, 2022.

[36] Y. Y. Guo, X. H. He, H. L. Li, B. Liu, S. C. Liu, and H. Z. Qi, "The use of the general thermal sensation discriminant model based on CNN for room temperature regulation by online brain-computer interface," *Building and Environment*, vol. 241, article 110494, 2023.

[37] X. Xu, L. Zhao, and Z. Yang, "Field experimental investigation on human thermal comfort in vehicle cabin," in *SAE Technical Paper Series*, March 2022.

[38] S. Sanei and J. A. Chambers, *EEG Signal Processing*, Wiley, 2013.

[39] R. W. Homan, J. Herman, and P. Purdy, "Cerebral location of international 10-20 system electrode placement," *Electroencephalography and Clinical Neurophysiology*, vol. 66, no. 4, pp. 376–382, 1987.

[40] Y. Jiao, X. Wang, Y. Kang, Z. Zhong, and W. Chen, "A quick identification model for assessing human anxiety and thermal comfort based on physiological signals in a hot and humid working environment," *International Journal of Industrial Ergonomics*, vol. 94, article 103423, 2023.